

# Evolution of Vehicle Exhaust Particles in the Atmosphere

Manjula R. Canagaratna, Timothy B. Onasch, Ezra C. Wood, Scott C. Herndon, John T. Jayne, Eben S. Cross, Richard C. Miake-Lye, Charles E. Kolb, and Douglas R. Worsnop  
*Aerodyne Research, Inc., Billerica, MA*

## ABSTRACT

Aerosol mass spectrometer (AMS) measurements are used to characterize the evolution of exhaust particulate matter (PM) properties near and downwind of vehicle sources. The AMS provides time-resolved chemically speciated mass loadings and mass-weighted size distributions of nonrefractory PM smaller than 1  $\mu\text{m}$  (NRPM<sub>1</sub>). Source measurements of aircraft PM show that black carbon particles inhibit nucleation by serving as condensation sinks for the volatile and semi-volatile exhaust gases. Real-world source measurements of ground vehicle PM are obtained by deploying an AMS aboard a mobile laboratory. Characteristic features of the exhaust PM chemical composition and size distribution are discussed. PM mass and number concentrations are used with above-background gas-phase carbon dioxide (CO<sub>2</sub>) concentrations to calculate on-road emission factors for individual vehicles. Highly variable ratios between particle number and mass concentrations are observed for individual vehicles. NRPM<sub>1</sub> mass emission factors measured for on-road diesel vehicles are approximately 50% lower than those from dynamometer studies. Factor analysis of AMS data (FA-AMS) is applied for the first time to map variations in exhaust PM mass downwind of a highway. In this study, above-background vehicle PM concentrations are highest close to the highway and decrease by a factor of 2 by 200 m away from the highway. Comparison with the gas-phase CO<sub>2</sub> concentrations indicates that these vehicle PM mass gradients are largely driven by dilution. Secondary aerosol species do not show a similar gradient in absolute mass concentrations; thus, their relative contribution to total ambient PM mass concentrations increases as a function of distance from the highway. FA-AMS of single particle and ensemble data at an urban receptor site

shows that condensation of these secondary aerosol species onto vehicle exhaust particles results in spatial and temporal evolution of the size and composition of vehicle exhaust PM on urban and regional scales.

## INTRODUCTION

Vehicle emissions represent large sources of atmospheric gaseous and particulate pollution. On regional and global scales, the black carbon (BC) in vehicular particulate matter (PM) emissions plays a potentially important role in climate forcing.<sup>1</sup> On the local scale, PM emissions from vehicles affect urban air quality and visibility<sup>2</sup> and have been linked to adverse health effects.<sup>3</sup> In light of their detrimental impacts, the U.S. Environmental Protection Agency (EPA) has instituted emission standards that regulate PM mass, which is viewed as the best currently available indicator of adverse health effects.

The local, regional, and global impacts of vehicle emission sources are intimately linked to the properties of the PM they produce. Thus, there is a need for detailed characterization of vehicle exhaust PM properties. To address EPA emission regulations, there is a particular need for quantification and characterization of the mass concentrations, chemical composition, and size distributions of emission particles. Previous studies have shown that vehicle exhaust PM can be broadly divided into a nanoparticle mode ( $d < 50$  nm) and an accumulation mode ( $50$  nm  $< d < 1000$  nm).<sup>4</sup> Gasoline and diesel vehicles produce nanoparticles, whereas accumulation-mode emissions are typically more abundant in diesel emissions. Nanoparticles contain sulfate and semi-volatile organic species and are formed by nucleation processes in the exhaust plume.<sup>5,6</sup> On the other hand, accumulation-mode particles consist of soot cores that are directly produced in the engine and are subsequently coated with sulfate and semi-volatile organic species in the exhaust plume.<sup>7</sup> Sulfate emitted by current diesel vehicles is typically lower than that observed in older measurements because of the dramatically lower sulfur content in diesel fuels since 2006.<sup>7</sup>

A challenge associated with exhaust PM measurement is the dynamic character of exhaust PM. When hot exhaust plumes are emitted into and mix with ambient air, they undergo rapid cooling that causes volatile and semi-volatile exhaust species to repartition between the gas and particle phases according to the extent of exhaust plume dilution and cooling. During plume dilution, there is an evolving competition among new particle formation (via nucleation), particle growth (via condensation and coagulation), and reduction of particle size and mass (via

## IMPLICATIONS

Predictions of vehicle PM effects depend on detailed understanding of their evolving properties on local, regional, and global scales. AMS measurements were used to characterize variations in mass concentrations, chemical composition, and size distributions of vehicle PM as a function of exhaust plume dilution and processing under real-world conditions. A key component of this work is FA-AMS data, which allow for direct quantification of vehicular source PM in an ambient environment. This represents an improvement over tracer-based apportionment methods, which require a priori knowledge of exhaust PM source signatures and large scaling factors.

evaporation). Thus, the measured chemical and physical properties of PM in a diluting exhaust plume is highly dependent on where, when, and how the given measurement is made. For example, nanoparticle formation in vehicle exhaust has been shown to be highly variable and critically dependent on the details of the plume dilution process (i.e., rate of dilution, dilution ratio, and dilution temperature).<sup>8–11</sup> Evolution of nanoparticle concentrations and size distributions has also been observed downwind of highways and motorways.<sup>12</sup>

Dilution and atmospheric processing of the exhaust plume are expected to cause continued variations in vehicle emission PM mass concentrations and size-dependent composition downwind of the emission source. For example, evaporative repartitioning<sup>11,13</sup> provides a mechanism for continued evolution of exhaust PM properties; it may also provide a source of gas-phase precursor species for ambient secondary organic material downwind of source regions.<sup>14</sup> As exhaust PM is transported from source regions to urban and regional spatial scales, the soot containing accumulation-mode exhaust particles, which have long atmospheric lifetimes, can also interact with other aerosol- and gas-phase species through coagulation and condensation processes. These interactions can transform the externally mixed, hydrophobic, and fractal soot particles into internally mixed, more hygroscopic, and more spherical particles.<sup>15</sup> The time and length scales for these transformations are key uncertainties in the prediction of the local, regional, and global impacts of exhaust PM.

In light of their continuous evolution, there is a need to measure the properties of vehicle emission particles throughout their atmospheric lifetimes under real-world conditions. Source PM measurements obtained under on-road conditions are needed to more accurately interpret and parameterize the dynamometer-based PM measurements and emission inventories used in air quality models. Measurements of vehicle PM properties at receptor sites are also needed to evaluate air quality model predictions, assess the effectiveness of control strategies, and estimate vehicle-PM-related impacts. Different approaches have been used to measure vehicle exhaust PM under realistic emission and dilution conditions. Tunnel and roadside emission studies allow for sampling ensemble properties of vehicles under specific driving, dilution, temperature, and humidity conditions<sup>16–18</sup>; mobile laboratories equipped with highly time-resolved PM and gas-phase measurements allow for on-road vehicle emission measurements.<sup>19–25</sup> From the standpoint of receptor measurements, the transformation of exhaust PM as it is transported away from its emission source can be characterized by studies at selected fixed locations downwind of a roadway and in mixed urban and regional ambient environments. Spatially resolved PM measurements downwind of source regions can also be obtained with mobile laboratories.<sup>26,27</sup>

Interpretation of data obtained under real-world operation conditions is complicated by the fact that the measured PM contains contributions not only from vehicle exhaust PM but also from nonvehicle-related primary and secondary PM sources. Interference from nonvehicle-related PM sources is particularly strong in particle mass

and composition measurements at receptor sites downwind of source regions. Historically, tracer-based apportionment methods<sup>28–30</sup> have been used for extracting vehicle emission contributions to ambient PM mass. These methods are limited by the fact that the tracers themselves only account for a small fraction of the exhaust PM mass concentration and the tracer/source profile relationships are highly variable.<sup>31</sup> Methods of apportioning vehicle PM mass concentrations on the basis of representative vehicle emission organic carbon/elemental carbon ratios have also been explored.<sup>32</sup> The variability of these ratios and other primary sources of elemental carbon also limit the effectiveness of this apportionment technique.<sup>33</sup>

In recent years, the aerosol mass spectrometer (AMS) has been used to obtain quantitative measurements of the mass concentrations and chemically speciated size distributions of nonrefractory particulate matter smaller than 1  $\mu\text{m}$  (NRPM<sub>1</sub>).<sup>34,35</sup> Multivariate factor analysis (FA) of AMS (FA-AMS) has been applied across many worldwide ambient sites and has been particularly effective at apportioning ambient organic PM mass into hydrocarbon-like organic aerosol (HOA) and oxygenated organic aerosol (OOA).<sup>36,37</sup> At most sites HOA and OOA correspond to primary organic aerosol (POA) and secondary organic aerosol (SOA) contributions to ambient aerosol, respectively. For example, comparisons of FA-derived POA mass concentrations and chemical mass balance-derived POA mass concentrations during the 2005 Study of Organic Aerosols in Riverside are within 15–20% of each other.<sup>38</sup> The dominant POA source in most sites is ground vehicle emissions. In cases in which the POA has large contributions from sources other than vehicle emissions (e.g., biomass burning) and cooking aerosol, the contributions of those sources have also been appropriately identified.<sup>39–42</sup> A key advantage of the FA-AMS analysis is that it can track the whole nonrefractory mass associated with vehicle PM without the need for a priori information or assumptions about the vehicle PM composition.

In this paper, AMS measurements are used to characterize the evolution of vehicle PM properties after emission into the atmosphere. The discussion in this paper is divided into two parts. The first part focuses on near-source measurements of aircraft and ground vehicle emission plumes. The aircraft plume measurements are used as a general case study for investigating the competition between nucleation and condensation in a hot exhaust plume as it dilutes and cools in ambient air. Mobile laboratory-based vehicle chasing experiments are used to measure ground vehicle PM emissions under real-world operation and dilution conditions. During these measurements, the high time resolution measurement capability of the AMS is used with gas-phase carbon dioxide (CO<sub>2</sub>) measurements to obtain on-road PM mass emission indices (EIs), size distributions, and compositions in individual vehicle plumes. The second part of the paper presents vehicle PM measurements obtained downwind of source regions. FA-AMS results from a gradient mapping study are used to investigate spatial gradients in organic aerosol composition and mass concentrations obtained immediately downwind of a highway. Fixed site measurements at a mixed urban receptor site illustrate the

effects of secondary ambient species on the size and chemical composition of primary vehicle emission particles on urban and regional scales.

## EXPERIMENTAL METHODS

The data presented in this paper were obtained over several different measurement campaigns. Experimental details for each of the measurement campaigns can be found in the following manuscripts: Aircraft Particle Emissions Experiment (APEX<sup>43</sup>), PM<sub>2.5</sub> Technology Assessment and Characterization Study in New York City (PMTACS-NY<sup>24</sup>), Somerville Highway Gradient Study,<sup>44</sup> and Megacity Initiative: Local and Global Research Observations (MILAGRO<sup>45</sup>). During these campaigns, a commercial TSI Model 3022 condensation particle counter (CPC) was used to obtain total number densities for particles with diameters between 7 and 2500 nm. BC measurements were obtained with a modified multiangle aerosol photometer. The BC measurements provide information about the soot-containing mode of vehicle exhaust. A commercial LICOR nondispersive infrared unit was used to obtain real-time CO<sub>2</sub> measurements. A description of the Aerodyne mobile laboratory used in the vehicle chase and mapping experiments is available in previously published manuscripts.<sup>23,24</sup>

Detailed descriptions of the AMS and its operation are available in several manuscripts.<sup>34,35</sup> Thus, only a brief summary of the instrument is given here. The AMS operates by using an aerodynamic lens to sample submicron particles into vacuum, where they are aerodynamically sized, thermally vaporized on a heated surface, and chemically analyzed via electron impact ionization mass spectrometry. The AMS provides size-dependent mass concentrations of NRPM<sub>1</sub>. Here, the term “refractory” is used to refer to material such as BC and metals that do not vaporize at the AMS vaporizer temperature of 600 °C. The particle size cutoffs for the AMS are determined by the lens transmission efficiency. The lens has 100% transmission for particles with vacuum aerodynamic diameters in the 70- to 500-nm size range. For particles with vacuum aerodynamic diameters of 1 μm, the transmission efficiency is approximately 50%. From the standpoint of vehicle PM measurements, the AMS provides quantitative mass concentration measurements of the accumulation-mode exhaust particles. Because of size cutoffs introduced by the inlet, the AMS cannot provide quantitative detection of the entire nanoparticle mode of vehicle exhaust PM. The AMS does display sharply reduced but non-zero sensitivity to the large end of the nanoparticle distribution (vacuum aerodynamic diameter >20–50 nm), which can be used to obtain qualitative information about trends in the nanoparticle mode.

AMS measurements provide chemically speciated mass concentrations and mass-weighted size distributions as a function of particle vacuum aerodynamic diameters ( $d_{va}$ ).  $d_{va}$  is defined as follows:

$$d_{va} = \frac{\rho_p}{\rho_0} \frac{d_{ve}}{\chi_v} = \rho_{eff} d_{ve} \quad (1)$$

Here,  $d_{ve}$  is the physical diameter of the spherical particle that would result if the nonspherical particle of interest were melted into a sphere while preserving any internal

void spaces. The shape factor,  $\chi_v$ , is defined as 1 for spherical particles and greater than 1 for aspherical particles. For a spherical particle, the effective density,  $\rho_{eff}$ , is the particle density,  $\rho_p$ ; for a nonspherical particle, the degree to which  $\rho_{eff}$  differs from  $\rho_p$  depends on its shape factor.  $\rho_0$  is the unit density.

A more detailed discussion of  $\rho_{eff}$  and a comparison to other  $\rho_{eff}$  definitions in the literature is available in DeCarlo et al.<sup>46</sup> AMS instruments fitted with internal light-scattering (LS) probes have been used to determine particle  $\rho_{eff}$ .<sup>47</sup> The LS probe is used to detect and optically size single particles. During typical operation, the LS-AMS is alternated between the traditional AMS operating mode, which provides size and composition information for the ensemble aerosol, and LS mode, which provides size and chemical composition information for single particles. For each particle that is detected in the LS mode, an optical diameter ( $d_{opt}$ ) is estimated and a  $d_{va}$  is obtained. The ratio between  $d_{va}$  and  $d_{opt}$  provides a measure of the particle  $\rho_{eff}$ .<sup>47</sup>

## RESULTS AND DISCUSSION

### Vehicle Emission Measurements Near the Source

*Aircraft Case Study.* Aircraft emissions represent a significant source of local particulate pollution, particularly in areas near and surrounding airports. The exhaust plume conditions of aircraft vehicle emission sources are different from those of ground vehicles. However, they share common PM constituents that are likely to display qualitatively similar microphysical trends in the diluting exhaust plumes. Thus, the aircraft plume measurements presented here provide a case study for investigating evolution of exhaust PM properties during the atmospheric dilution of a hot exhaust plume.

Onasch and co-workers<sup>43</sup> have characterized exhaust emissions from a stationary aircraft as a function of distance from the engine exit plane and as a function of engine power. The aircraft was tethered in place on the ground, and the aircraft engine was operated at a range of power settings ranging from idle/taxi to take-off conditions while the evolution of exhaust particle number, size, mass, and chemical composition was measured. The aircraft exhaust was sampled through probes that were placed at 1, 10, and 30 m downstream of the engine exit plane. These measurements were obtained as part of APEX and are described in more detail in a previous publication.<sup>43</sup>

Figure 1 presents mass emission factors (EF<sub>m</sub>) and number emission factors (EF<sub>n</sub>) measured with PM measurements at the 30-m probe distance. Measurements for a range of engine power conditions are shown. EFs are calculated by normalizing the mass or number concentrations to the estimated mass of fuel burned. Figure 1a shows the AMS size-dependent distribution of EF<sub>m</sub>. The distribution is trimodal. The ambient mode (~350 nm) reflects background ambient PM, the condensation mode (~250 nm) consists of volatile/semi-volatile exhaust components condensed on BC, and the nucleation mode (~35 nm) consists of volatile/semi-volatile exhaust components. As in ground vehicle exhaust, the condensed nonrefractory material in both exhaust PM modes consists of sulfuric acid and organic species. Figure 1b shows that the changing size distributions are not

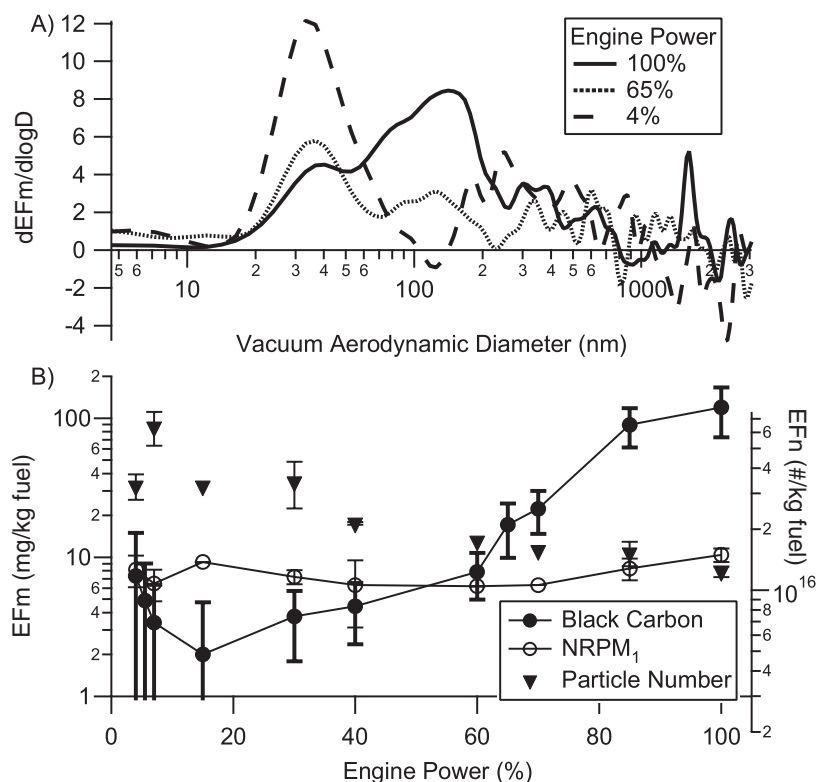


**Figure 1.** (A) Size distributions of EF<sub>m</sub> measured with the AMS at a probe distance of 30 m and at engine powers of 4, 65, and 100%. (B) Engine power dependence of EF<sub>n</sub> and BC and NRPM<sub>1</sub> EF<sub>m</sub> at a probe distance of 30 m. The EFs are calculated by normalizing the mass or number concentrations to the estimated mass of fuel burned.

linked with any trends in NRPM<sub>1</sub>, but they do correlate with engine-power-dependent changes in particle number and BC emission factors (EFs).

Taken together, the observations in Figure 1, a and b, illustrate the competition between condensation and nucleation processes in the exhaust plume. In general, nucleation processes are favored when the particle surface area available for condensation (i.e., condensational sink) is low. On the other hand, condensation-driven growth is observed when the condensational sink is high. Refractory BC emissions represent a significant condensational sink for volatile and semi-volatile species in exhaust plumes. Thus, at the highest engine powers when BC emissions are the highest, the nucleation mode becomes suppressed relative to the condensation mode and low particle number concentrations are observed. On the other hand, at low engine powers when BC emissions are low, the nucleation process is dominant and a more intense nucleation mode and higher particle number concentrations are observed.

**On-Road Ground Vehicle Measurements.** Mobile laboratories equipped with highly time-resolved PM and gas-phase measurements are used to obtain on-road vehicle emission measurements.<sup>19–23</sup> In particular, mobile laboratory-based vehicle chasing experiments provide a unique means of measuring on-road emissions from individual vehicles under real-world operation and dilution conditions. Figure 2 shows an example of data obtained while chasing an individual diesel vehicle with the Aerodyne mobile laboratory in New York City as part of the

PMTACS-NY campaign in 2001.<sup>24</sup> These results were obtained while following the target vehicle at distances ranging from 3 to 15 m. Figure 2 shows the time trends of PM mass concentration, particle number concentrations, and CO<sub>2</sub> concentrations ([CO<sub>2</sub>]) measured during this chase. The PM mass concentrations were obtained with an AMS, and the number concentrations were obtained with a CPC.

In this study, gas-phase [CO<sub>2</sub>] is used as a dilution tracer of the vehicle emission plume. CO<sub>2</sub> is ideal for this purpose because it is chemically inert and it has a well-defined EF that can be used to determine the extent of plume dilution and to calculate fuel-use-based EFs for the various PM properties. The correlated increases in the particle and [CO<sub>2</sub>] are evident in Figure 2a. The simultaneous peaks in the particle and [CO<sub>2</sub>], which usually last for approximately 10–20 sec, are plume captures, which represent separate instances during the chase when the sampling inlet of the mobile laboratory captured the target vehicle's exhaust plume. Video camera images and operator notes obtained during each chase event were used to remove measurement time periods that were contaminated by other on-road vehicles and sources. The baseline signal levels in the gas and particle time trends represent time periods when ambient roadway background concentrations of the various species were sampled. Concentrations of CO<sub>2</sub> in excess of background CO<sub>2</sub> (CO<sub>2</sub> – CO<sub>2</sub> <sub>bgd</sub>) ranged from 100 to 800 parts per million (ppm). On the basis of exhaust [CO<sub>2</sub>] in diesel and gasoline vehicles, this corresponds

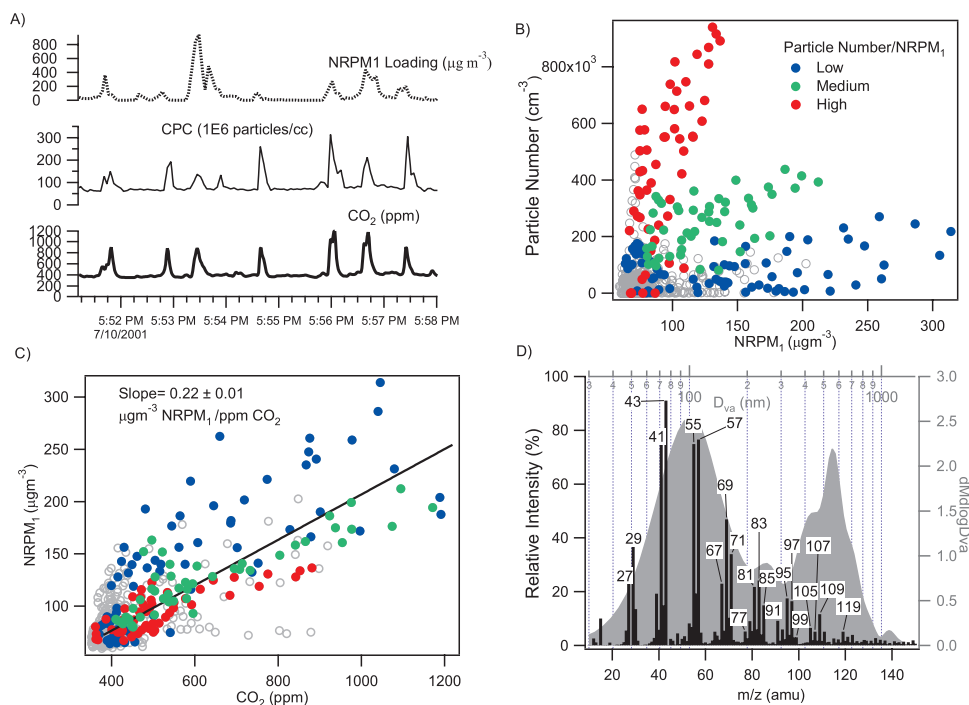


**Figure 2.** (A) Results from an individual diesel vehicle chase during the PMTACS-NY study. Time-resolved measurements of NRPM<sub>1</sub> mass (AMS), particle number (CPC), and gas-phase CO<sub>2</sub> (LICOR) were obtained during the chase. (B) Ratios between the particle number and NRPM<sub>1</sub> measurements shown in panel A. Plume captures from the chase that display low, medium, and high ratios are highlighted for reference. (C) NRPM<sub>1</sub> mass concentrations vs. [CO<sub>2</sub>]. The slope of the plot is related to the fuel-based EFs. Datapoints are colored according to their particle number to NRPM<sub>1</sub> as in panel B. (D) Exhaust PM mass spectrum and mass-weighted size distribution averaged over all diesel chase events.

to plume dilution ratios of 25–1000 at the point of measurement.

Figure 2b compares the particle mass and number concentrations emitted by the target diesel vehicle in Figure 2a. Variable particle number-to-mass ratios are observed. Individual plume captures that show low, medium, and high ratios between particle number and NRPM<sub>1</sub> are colored in the figure for reference. In Figure 2c, NRPM<sub>1</sub> mass emissions are plotted against exhaust [CO<sub>2</sub>], a surrogate for plume dilution. Plume captures are colored according to their particle number-to-mass ratios in Figure 2b. High, medium, and low ratios are observed across all plume dilution levels, indicating that the observed variability in particle number-to-mass ratios does not have a strong correlation with plume dilution alone. The aircraft case study described above shows that particle number emissions are affected by the BC present in the exhaust plume. BC emissions were not measured in the chase study, but BC is expected to provide the main condensation sink in the diesel exhaust stream.<sup>7</sup> Previous studies have shown that heavy-duty diesel trucks that emit large amounts of BC do not emit high particle numbers and vice versa.<sup>48</sup> Thus, the observed dynamic variability between particle number and NRPM<sub>1</sub> emissions could be a result of varying BC emissions during on-road operation of the target vehicle.

Because [CO<sub>2</sub>] can be directly related to the amount of fuel burned, the slope of Figure 2c is the average NRPM<sub>1</sub> EF<sub>m</sub> of the target vehicle. The slope in Figure 2c is  $0.22 \pm 0.01 \mu\text{g m}^{-3}/\text{ppm CO}_2$ , which corresponds to an NRPM<sub>1</sub> EF of 0.39 g/kg fuel. The scatter around the average slope is larger than the measurement uncertainty and, as discussed above, likely reflects the inherent variability in

mass EIs because of changing on-road operating and dilution conditions. During the New York City study, on-road EIs were obtained for several individual diesel trucks and buses. When taken together, these results provide average EFs for each vehicle type. An average NRPM<sub>1</sub> EF of 0.37 g/kg fuel was obtained for 20 individual truck chases. The NRPM<sub>1</sub> EF obtained from 141 individual diesel buses ranged from 0.122 to 0.25 g/kg fuel depending on the particular engine type used by the bus.<sup>24</sup> Schneider and co-workers have also reported chase study measurements of NRPM<sub>1</sub> EFs for 18 motorway trucks that average approximately 0.125 g/kg fuel.<sup>27</sup> Tunnel measurements show NRPM<sub>2.5</sub> (NRPM ≤ 2.5 μm in size) EF<sub>m</sub> for trucks of 0.5 g/kg fuel.<sup>17</sup> In comparable dynamometer studies, NRPM<sub>2.5</sub> EF<sub>m</sub> from trucks range from 0.4 to 0.9 g/kg fuel<sup>49,50</sup> and NRPM<sub>2.5</sub> EF<sub>m</sub> from buses range from 0.3 to 0.6 g/kg fuel.<sup>51</sup> The conversion factors and assumptions used to convert between the various EF units measured in these studies are described in the paper by Canagaratna and co-workers.<sup>24</sup>

When taken together, the on-road measurements appear to be systematically lower by approximately 50% than the dynamometer measurements obtained for diesel buses and trucks. Although some of these differences could be due to biases in the measurement techniques (i.e., NRPM<sub>1</sub> vs. NRPM<sub>2.5</sub> or positive artifacts in dynamometer filter measurements), it is also possible that at least some of the observed differences are due to differences in plume dilution. Recent studies have shown that repartitioning of semi-volatile species during the plume dilution process can have a significant effect on measured PM EF<sub>m</sub>.<sup>13</sup> For example, emission studies of diesel engines

show that changing the exhaust dilution ratio from 20:1 to 350:1 does not affect soot emissions, but it decreases the measured organic aerosol mass by as much as 50%.<sup>13</sup> More intercomparisons among real-world and dynamometer EF measurements are needed to better characterize this effect.

*On-Road Measurements of PM Chemical and Physical Properties.* During the PMTACS-NY measurement campaign discussed above, the AMS aboard the mobile laboratory provided complete mass spectra and mass-weighted size distributions every 2 sec. Figure 2d shows the background-corrected mass spectrum obtained by averaging over the exhaust PM data obtained from all individual diesel vehicle chases. Before the individual chase mass spectra were averaged together, the appropriate ambient background mass spectrum was subtracted from the average chase mass spectrum for each chase. The mass spectrum in Figure 2d is dominated by ion series such as  $C_nH_{2n+1}^+$  ( $m/z$  29, 43, 57, 71, 85, 99...),  $C_nH_{2n-1}^+$  ( $m/z$  27, 41, 55, 69, 83, 97, 111...), and  $C_nH_{2n-3}^+$  ( $m/z$  67, 79, 81, 95, 107, 109...). These ion series are characteristic of saturated hydrocarbons, branched alkanes and alkenes, and cycloalkanes, respectively. Comparisons between the spectra in Figure 2d and reference fuel and oil spectra indicate that lubricating oil dominates the exhaust NRPM composition. A small contribution from sulfuric acid is also observed.<sup>24</sup> These results are consistent with off-line gas chromatography–mass spectrometry analysis,<sup>29</sup> online exhaust measurements performed under laboratory settings,<sup>5,52</sup> and other dynamometer and on-road AMS measurements.<sup>53</sup>

In the chase measurements, the ratio between organic and sulfuric acid species was observed to vary among diesel vehicles. However, the relative ratios of the various organic ion series observed in Figure 2d did not show any significant variability with plume  $[CO_2]$  (i.e., dilution ratio) or among diesel vehicles. This is consistent with the observations of Sakurai et al.,<sup>6</sup> which showed that the lubricating oil species in diesel particles have similar volatility profiles irrespective of engine load, fuel, and particle size. This indicates that although the NRPM mass EIs of diesel vehicles may vary with dilution and operating conditions, the composition of the NRPM that contributes to the observed mass EI may be less sensitive to these conditions. It is useful to note that different results may be observed for vehicles fitted with new exhaust aftertreatment devices. Most aftertreatment devices oxidize exhaust species. Although oxidizing the exhaust reduces the overall organic PM mass loadings, it also has the potential to yield a larger dynamic range of oxidized organic species with varying volatilities in vehicle exhaust. This could produce chemical composition differences between roadway and dynamometer studies with vehicles with aftertreatment technology.

Figure 2d shows the AMS NRPM<sub>1</sub> size distributions averaged over all diesel vehicle chase measurements. The average size distribution in Figure 2d was obtained after the background aerosol size distribution was subtracted from the average vehicle plume size distributions for each individual chase. Because AMS size distributions are weighted by mass, the accumulation mode of exhaust PM in Figure 2d is more dominant than the nanoparticle mode. The nanoparticle-mode contribution to this size distribution is further reduced

in this study by low transmission efficiencies of nanoparticles into the AMS. Schneider et al.<sup>53</sup> have shown that AMS size distributions of exhaust PM measured under roadway, chase, and dynamometer conditions are similar to that shown in Figure 2d.

The accumulation mode in Figure 2d consists of coated soot particles.<sup>7</sup> Experimental<sup>54</sup> and theoretical<sup>46</sup> studies by several groups have shown that for aspherical soot particles,  $d_{va}$  peaks at approximately 100 nm and is largely independent of particle size because of a correlated increase in particle shape factor and particle size (see eq 1). Although the AMS does not directly measure the soot cores of these particles, the measured  $d_{va}$  of the exhaust PM reflects the asphericity of the core. The fact that exhaust PM accumulation-mode size distributions peak at approximately 100 nm, regardless of the exact source measurement scenario (i.e., dynamometer, roadway, or chase conditions<sup>53</sup>) indicates that accumulation exhaust mode geometry is dominated by its aspherical soot core.

In Figure 2d, there is significant mass concentration in the 200- to 350-nm size range. Particles in this size range were not observed in dynamometer studies of exhaust PM<sup>53</sup> but were observed in other on-road truck measurements.<sup>27</sup> The canonical mass-weighted engine exhaust distribution of Kittleson et al.<sup>4</sup> shows a broad accumulation mode with significant mass concentration from 50 nm to nearly 1  $\mu$ m. Previous studies indicate that because of the increasing asphericity with soot particle size,<sup>46,54,55</sup> even soot particles with large physical diameters would exhibit  $d_{va}$  of approximately 100 nm. This suggests that the particles that fall in the 200- to 350-nm size range correspond to near-spherical particles that consist of heavily coated soot or even pure oil. The distinct particle mode in Figure 2d that starts at approximately the 350-nm mode cuts off at diameters greater than 500 nm because of reduced AMS inlet transmission efficiency at these particle sizes. This mode was not consistently observed in all chase events and likely corresponds to re-entrained particles that had been deposited on cylinder and exhaust system surfaces.<sup>4</sup>

### Vehicle Emission Measurements away from Source Regions

*Measurements Downwind of Roadways.* Measurements downwind of roadways can be obtained by using selected fixed locations downwind of a roadway or by using more detailed spatial mapping with mobile laboratories.<sup>26,27</sup> Figure 3 shows results from a mobile laboratory deployment designed to map the evolution of gas and particulate vehicle emissions downwind of Interstate-93, a major highway that runs through Somerville, MA.<sup>44</sup> The figure shows the spatial gradients in particle number concentrations observed during this campaign. The data were obtained on a single winter morning while the mobile laboratory was driven repeatedly along a prescribed loop that sampled air masses a series of distances downwind from the highway. In addition to the real-time particle number (CPC) measurements, an AMS was also deployed to obtain particle mass and chemical composition measurements. The gradient measurements shown here were carried out during the morning hours to maximize the rush hour impact of vehicle emissions while minimizing the effect of photochemistry on the observed aerosol.



**Figure 3.** Particle number concentrations measured with a CPC downwind of major roadways and highways in Somerville, MA. These measurements were obtained with the Aerodyne mobile laboratory.

In Figure 3, there is a clear decrease in CPC number concentrations away from the roadway source regions. This is consistent with the fact that in urban areas vehicle emissions are key contributors to particle number concentrations.<sup>56</sup> Because nonvehicle-related sources can have a larger effect on the measured particle mass concentrations, FA-AMS analysis is used to apportion the AMS mass concentrations observed during the mapping measurements. The FA-AMS analysis is performed with the positive matrix factorization evaluation tool and according to methods presented by Ulbrich and co-workers.<sup>57</sup> Two main components (HOA and OOA) are obtained. The spatial variation in HOA and OOA mass loadings is shown in Figure 4. The HOA component has a strong correlation with carbon monoxide and nitrogen oxides and a mass spectrum that resembles that shown in Figure 2d. AMS mass spectra obtained from diesel and gasoline vehicles do not differ significantly from each other and cannot be directly separated with FA-AMS. Thus, the HOA concentrations in Figure 3 correspond to contributions from diesel and gasoline vehicles.

Spatial gradients of gas-phase  $\text{CO}_2$  are shown in Figure 4a. It is clear from the figure that the  $\text{CO}_2$  spatial distribution is similar to that of HOA. This is consistent with the interpretation that HOA has a roadway vehicle source and that its observed gradient in mass concentration is largely determined by dilution. The lack of any significant spatial gradient in OOA indicates that OOA corresponds to aged background aerosol. Although the ambient PM mass concentrations measured close to the highway in this study were dominated by exhaust PM, by 200 m the aged background aerosol contributed as much to the ambient PM mass as vehicle PM. This observation highlights the need for FA methods when interpreting

total organic mass concentration measurements obtained even a short distance away from the emission source. The ability to observe roadway-induced gradients in total organic PM mass concentrations depends on the ratio between the primary vehicle PM (HOA) and secondary (OOA) aerosol mass concentrations. In environments with high background OOA concentrations, variations due to HOA gradients may not be detectable without a technique such as FA-AMS. This may be an explanation for some gradient measurements that show sharp decreases in BC concentrations away from the highway even while measured changes in PM mass concentrations are minimal.<sup>27</sup> This is also consistent with a recent multivariate regression analysis of data measured near a freeway that found a positive correlation between the particle volume in the accumulation and solar radiation, indicating that the contributions to the accumulation mode from secondary species is not negligible.<sup>12</sup>

The above-background excess  $[\text{CO}_2]$  measured in the mapping studies are much lower than those typically observed during the chase study shown in Figure 2. However, there is still a clear correlation between  $\text{CO}_2$  and HOA that can be used to obtain an average EF for the mixed vehicle fleet sampled during these measurements. Figure 4b shows the correlation between background-subtracted values of HOA and  $\text{CO}_2$ . HOA and  $\text{CO}_2$  values measured at 300 m were used as background values. The plot shows literature values for EF from gasoline vehicles ( $\text{EF}_{\text{gas}}$ ) and diesel vehicles ( $\text{EF}_{\text{diesel}}$ ).<sup>24,58</sup> The measured datapoints reflect an average fleet EF that lies between the guidelines defined by  $\text{EF}_{\text{gas}}$  and a weighted sum of  $\text{EF}_{\text{gas}}$  and  $\text{EF}_{\text{diesel}}$  ( $90\%\text{EF}_{\text{gas}} + 10\%\text{EF}_{\text{diesel}}$ ). Because the on-road fleets of gasoline and diesel vehicles do not burn the same volume of fuel and emit

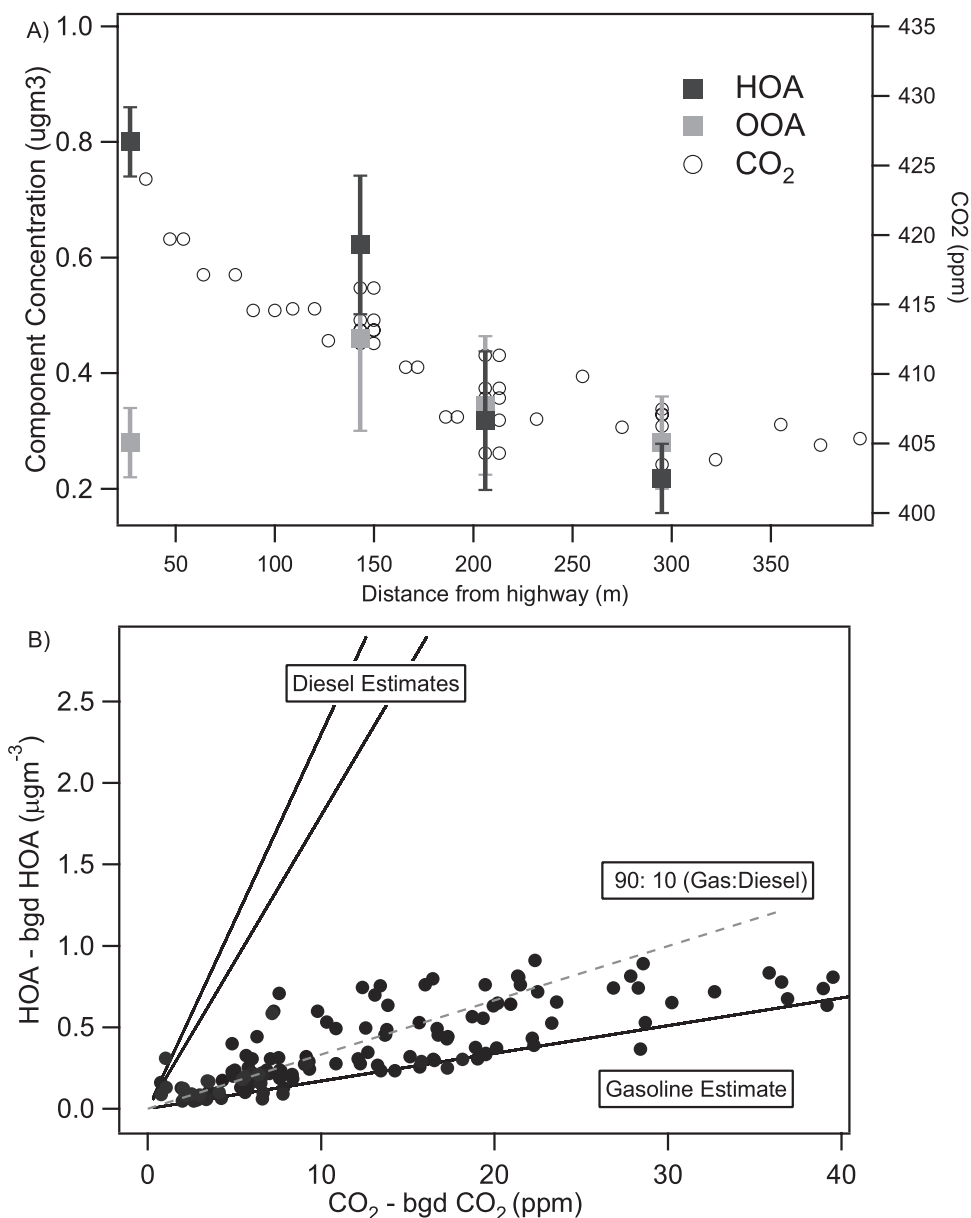


**Figure 4.** Particle mass and [CO<sub>2</sub>] observed downwind of major roadways and highways in Somerville, MA. (A) The particle mass concentrations of the HOA component, which corresponds to the freshly emitted vehicle PM, and the OOA component, which corresponds to the aged background aerosol, are shown. Decreasing HOA and [CO<sub>2</sub>] with distance reflect the effects of dilution. (B) NRPM<sub>1</sub> mass concentrations vs. excess CO<sub>2</sub> above background levels (CO<sub>2</sub> - CO<sub>2</sub> bgd). Reference lines for gasoline and diesel EFs from Ban-Weiss<sup>58</sup> and diesel EFs from Canagaratna et al.<sup>24</sup> are shown. The dashed line corresponds to a weighted sum of the gasoline and diesel EFs. See text for more discussion.

the same amount of net CO<sub>2</sub> into the atmosphere, this simplistic top-down method cannot be used to apportion the measured average fleet EF to contributions from diesel and gasoline vehicles. However, these types of measurements provide valuable data for testing model predictions of emissions from mixed vehicle sources.

*Exhaust PM on Urban and Regional Scales.* As shown in Figure 4a, vehicle emission contributions to ambient PM mass concentrations decrease rapidly with distance from the vehicle source. An analysis by Zhang et al.<sup>37</sup> of multiple sites in the Northern Hemisphere also shows similar effects on urban and regional scales. In particular, the absolute mass concentrations of primary HOA components in the atmosphere decrease with distance from urban centers. Although

in the urban centers the HOA-to-organic-aerosol ratio is approximately 36% of the mass, this ratio decreases to 19 and 5% in urban-downwind and remote/rural environments, respectively. These studies show that secondary aerosol species account for a large fraction of the ambient PM in most environments. Given the importance of secondary species to ambient aerosol particles, it is useful to understand how these species affect the properties of primary vehicle emission particles. The dominant mechanisms for the formation of secondary aerosol species involve gas-phase photo-oxidation reactions. Once secondary species are formed in the gas phase, they can condense onto pre-existing ambient particles, including vehicle exhaust PM and aged background PM. As primary exhaust particles become coated with oxidized organic and inorganic species,

changes are induced in their chemical composition, density, and hygroscopic properties. The addition of coatings can also change the densities and shape factors of fractal exhaust particles.

Figure 5 shows results from LS-AMS measurements obtained at a mixed urban site in Mexico City.<sup>45</sup> During this study, 2956 individual ambient particles were detected with the LS probe and the AMS mass spectrometer. The single particle measurements in the LS mode were also alternated with AMS measurements of the ensemble-averaged ambient NRPM<sub>1</sub>. The particle statistics in LS mode were not high because this was an early deployment of the LS module coupled to an AMS with a time-of-flight mass spectrometer. Moreover, only particles with a  $d_{va}$  greater than 300 nm were detected because of the optical cutoff of the LS module. For each of the 2956 individual particles detected by LS signal, a complete mass spectrum was measured. Each single-particle mass spectrum was analyzed with FA, and the single particle was classified according to its HOA content. Single particles with HOA mass fraction more than 90% are categorized as HOA single particles, whereas those with HOA content less than 90% are categorized as mixed single particles. In the simple extreme, a single particle classified as HOA corresponds to fresh vehicle exhaust emission PM, whereas a single particle classified as mixed corresponds to PM with significant contributions from secondary aerosol (i.e.,

background aerosol particles, which include vehicle exhaust particles coated with secondary material).

Figure 5a shows the diurnal trends in number of classified HOA single particles and mixed single particles. The simultaneously measured diurnal trends of the ensemble-averaged HOA and particulate nitrate ( $\text{NO}_3^-$ ) mass concentrations are also shown. It is important to note when comparing these two types of measurements that the single particles measured with the LS probe correspond to only a small and limited ( $d_{va} > 300$  nm) subset of all of the NRPM<sub>1</sub> measured in the ensemble-averaging mode. In Figure 5, the hours from 12:00 to 9:00 a.m. are referred to as period A, and the hours from 9:00 a.m. to 12:00 p.m. are referred to period B. The HOA single-particle numbers and HOA ensemble mass concentrations are highest in the morning (period A) and evening hours, consistent with the urban traffic patterns around this site. During period B, significant ensemble HOA mass concentrations are observed, but the absolute number and fraction of single particles classified as HOA drop rapidly. This drop in the number fraction of HOA single particles correlates with a simultaneous and rapid increase of secondary  $\text{NO}_3^-$  in the ensemble NRPM<sub>1</sub>. This suggests that during period B,  $\text{NO}_3^-$  and other photochemically produced secondary species condense onto the fresh HOA single particles and transform them into mixed single particles.

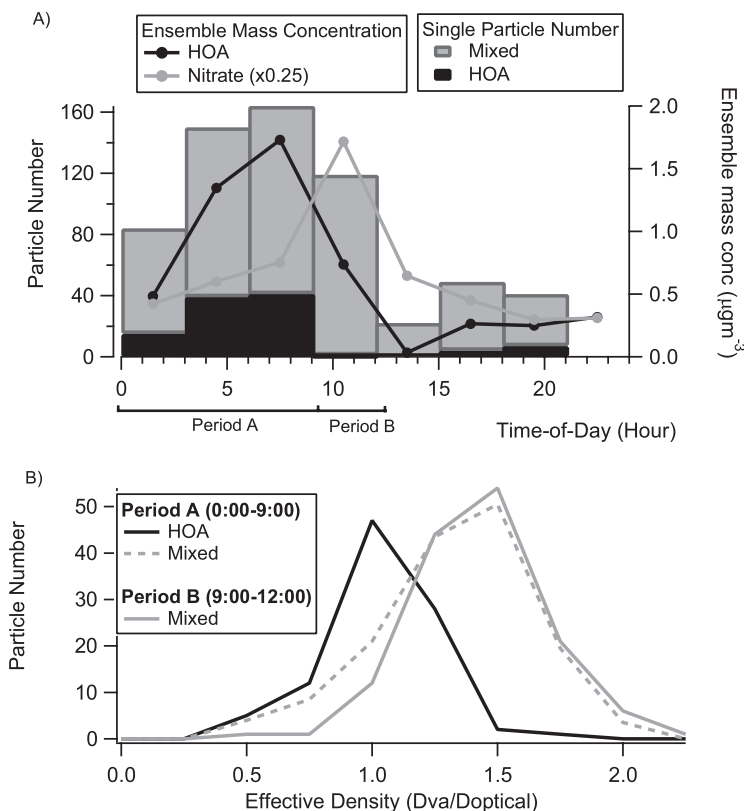


**Figure 5.** Single particle and ensemble data measured with a LS-AMS at a mixed urban site during the MILAGRO campaign. (A) Diurnal time trends in single particle number and ensemble particle mass concentrations. The organic components in the single-particle mass spectra and ensemble mass spectra were classified with FA. Single particles were classified as HOA or mixed according to their HOA content. The single particles represent a limited subset of all particles averaged together in the ensemble measurements. See text for more discussion. Two time periods of interest (A and B) are highlighted at the bottom of the figure. (B)  $\rho_{\text{eff}}$  distributions of the single particles shown in panel A during periods A and B.  $\rho_{\text{eff}}$  is calculated as the ratio between  $d_{va}$  and  $d_{\text{opt}}$ .

For each single particle detected by the LS module, a  $d_{\text{opt}}$  was estimated from the LS intensity and a  $d_{\text{va}}$  was measured from the particle time of flight. These data are used to calculate the distributions of particle  $\rho_{\text{eff}}$  observed during periods A and B (see Figure 5b). The observed  $\rho_{\text{eff}}$  distributions are consistent with the observation of HOA and mixed single particles during period A and the observation of only mixed particles during period B. The HOA single particles observed with the LS probe have  $d_{\text{va}}$  values of more than 300 nm, and as discussed earlier in the description of Figure 2d, it is likely that they are dominated by lubricating oil and have a more compact and spherical shape than the fractal vehicle emission particles that are observed at  $d_{\text{va}}$  values of approximately 100 nm. The density of lubricating oil is  $0.9 \text{ g cm}^{-3}$ . Thus, if a spherical shape is assumed for the HOA single particles, their estimated  $\rho_{\text{eff}}$  is approximately 0.9, which is in good agreement with the observed HOA particle  $\rho_{\text{eff}}$  of 1. On the basis of the ensemble average mass fractions observed during period B (i.e., 60% ammonium nitrate, 15% ammonium sulfate, and 25% organic), the density of the mixed particles is estimated to be  $1.6 \text{ g cm}^{-3}$ . Because the mixed particles are significantly aged, it is reasonable to assume that they are also spherical. The calculated  $\rho_{\text{eff}}$  of 1.6 for the mixed particles is also in good agreement with observed values. Taken together, the differences in the particle  $\rho_{\text{eff}}$  distributions measured during periods A and B are consistent with the hypothesis that the vehicle emission single particles detected in LS mode become mixed with and coated by secondary material during period B.

As noted earlier, the single particles detected in the LS mode are only a small and limited subset of all of the ambient particles detected in the ensemble averaging mode of the AMS. In fact, a large fraction of the ensemble HOA mass concentration in Figure 5a is due to coated fractal accumulation-mode soot particles that peak at  $d_{\text{va}}$  values of approximately 100 nm in Figure 2d. Although these particles were not directly measured with the LS mode, results from several previous studies suggest that they also evolve in a similar manner to the HOA single particles measured in this study. For example, AMS measurements by Zhang et al.<sup>59</sup> show that the OOA/HOA ratio of sub-100-nm particles increases diurnally with increasing ensemble OOA mass concentrations. Kleinman et al.<sup>60</sup> modeled the evolution of particle size distributions downwind of Mexico City and showed that the dominant source for increasing mass in the aged background aerosol mode is condensation-induced growth of the small mode particles. AMS size distributions measured in aged urban downwind or remote rural air masses contain a near-monomodal internally mixed background aerosol mode with little contribution from the externally mixed fractal soot mode that is observed in fresh urban air masses.<sup>15,61,62</sup> The study by Cubison and co-workers<sup>15</sup> used AMS measurements together with gas-phase measures of photochemical age to investigate the photochemical aging time scales of urban plumes. Their work indicates that although fresh urban air masses begin with externally mixed particles in the accumulation mode, these particles become internally mixed and more hygroscopic on the time scales of 1–2 days of atmospheric processing.

## CONCLUSIONS

The properties of vehicle emission PM evolve throughout their atmospheric lifetime. In this paper, AMS measurements are used to characterize the changes in exhaust PM properties that accompany exhaust plume dilution and atmospheric processing. Measurements are obtained near vehicle emission sources and downwind of emission source regions. AMS size distributions measured during an aircraft source study are used to investigate the microphysical changes that take place as volatile and semi-volatile gas-phase species partition between the gas and particle phase as the hot exhaust plume undergoes dilution and cooling. In these measurements, BC particles act as condensation sinks for the volatile and semi-volatile species and suppress nucleation processes in the exhaust. Ground vehicle exhaust PM chemical compositions and size distributions are measured under real-world dilution and operation conditions by deploying the AMS aboard a mobile laboratory. Correlations between simultaneously measured PM mass and gas-phase  $[\text{CO}_2]$  are used to identify vehicle plumes and to determine on-road vehicle  $\text{EF}_m$  for individual vehicles. On-road vehicle  $\text{EF}_m$  are approximately 50% lower than those estimated from dynamometer measurements. Although some of this systematic discrepancy may be due to differences in measurement size cutoffs ( $\text{PM} \leq 1 \text{ } \mu\text{m}$  vs.  $\text{PM} \leq 2.5 \text{ } \mu\text{m}$ ), enhanced evaporative repartitioning under the on-road dilution conditions may also play a role. Variability in the relationship between mass and number emissions is observed for individual vehicles and may be related to changing BC emissions during on-road operating conditions. FA is used to monitor and apportion the vehicle PM components in ambient AMS data that is measured downwind of a vehicle source. This analysis allows for direct quantification of vehicle PM mass concentrations without the need for the a priori knowledge of exhaust PM source signatures or large scaling factors that are typically required for tracer-based apportionment methods. Spatially resolved mapping measurements downwind of a highway show gradients in vehicle PM mass concentrations that decrease with distance from the source region. The mass concentrations of background SOA species do not change with distance from the highway. This results in an increasing relative contribution of SOA species as a function of distance from the vehicle emission source. AMS data at an urban receptor site show that temporal variations in the size and composition of exhaust PM are caused by condensation of secondary organic and inorganic species onto the vehicle exhaust particles. Continued condensation of the secondary species will eventually transform the exhaust PM, which is largely hydrophobic in nature when it is emitted, into a mixed hydrophilic organic and inorganic PM in mixed urban environments. This transformation has implications for the local and regional impacts of vehicle PM.

## ACKNOWLEDGMENTS

The authors gratefully acknowledge Nga L. Ng for help with preparation of figures and critical proofreading of the manuscript. APEX measurements were supported by funding from the University of Missouri Center of Excellence for Aerospace Particulate Emissions Reduction Research (National

Aeronautics and Space Administration Cooperative Agreement NCC3-1084) under University of Missouri–Rolla sub-contract number 000729-02. PMTACS-NY measurements were supported in part by the New York State Energy Research and Development Authority, contract number 4918ERTERES99; EPA Cooperative Agreement number R828060010; and the New York State Department of Environmental Conservation, contract number C004210. Funding from the Mystic View Task Force supported the Somerville gradient measurements. The MILAGRO measurements were funded by the Office of Science (BER); Department of Energy (Atmospheric Science Program) grant numbers DE-FG02-05ER63995, dE-FG02-05ER84268, and DOE DE-FG02-05ER63982; and Atmospheric Chemistry Program of the National Science Foundation grant number ATM-0525355.

## REFERENCES

- Jacobson, M.Z. Strong Radiative Heating due to the Mixing State of Black Carbon in Atmospheric Aerosols; *Nature* **2001**, *409*, 695-697.
- Watson, J.G. Visibility: Science and Regulation; *J. Air & Waste Manage. Assoc.* **2002**, *52*, 628-713.
- Pope, C.A.; Burnett, R.T.; Thun, M.J.; Calle, E.E.; Krewski, D.; Ito, K.; Thurston, G.D. Lung Cancer, Cardiopulmonary Mortality, and Long-Term Exposure to Fine Particulate Air Pollution; *J. Am. Med. Assoc.* **2002**, *287*, 1132-1141.
- Kittelson, D. Engines and Nanoparticles: A Review; *J. Aerosol Sci.* **1998**, *29*, 575-588.
- Sakurai, H.; Tobias, H.J.; Park, K.; Zarling, D.; Docherty, K.S.; Kittelson, D.B.; McMurry, P.H.; Ziemann, P.J. On-Line Measurements of Diesel Nanoparticle Composition and Volatility; *Atmos. Environ.* **2003**, *37*, 1199-1210.
- Tobias, H.J.; Beving, D.E.; Ziemann, P.J.; Sakurai, H.; Zuk, M.; McMurry, P.; Zarling, D.; Waytulonis, R.; Kittelson, D.B. Chemical Analysis of Diesel Engine Nanoparticles Using a Nano-DMA/Thermal Desorption Particle Beam Mass Spectrometer; *Environ. Sci. Technol.* **2001**, *35*, 2233-2243.
- Marić, M.M. Chemical Characterization of Particulate Emissions from Diesel Engines: a Review; *J. Aerosol Sci.* **2007**, *38*, 1079-1118.
- Morawska, L.; Ristovski, Z.; Jayaratne, E.R.; Keogh, D.U.; Ling, X. Ambient Nano- and Ultrafine Particles from Motor Vehicle Emissions: Characteristics, Ambient Processing and Implications on Human Exposure; *Atmos. Environ.* **2008**, *42*, 8113-8138.
- Zhang, K.M.; Wexler, A.S. Evolution of Particle Number Distribution near Roadways—Part I: Analysis of Aerosol Dynamics and Its Implications for Engine Emission Measurement; *Atmos. Environ.* **2004**, *38*, 6643-6653.
- Jacobson, M.Z.; Seinfeld, J.H. Evolution of Nanoparticle Size and Mixing State near the Point of Emission; *Atmos. Environ.* **2004**, *38*, 1839-1850.
- Jacobson, M.Z.; Kittelson, D.B.; Watts, W.F. Enhanced Coagulation Due to Evaporation and Its Effect on Nanoparticle Evolution; *Environ. Sci. Technol.* **2005**, *39*, 9486-9492.
- Ntziachristos, L.; Ning, Z.; Geller, M.D.; Sioutas, C. Particle Concentration and Characteristics near a Major Freeway with Heavy-Duty Diesel Traffic; *Environ. Sci. Technol.* **2007**, *41*, 2223-2230.
- Lipsky, E.M.; Robinson, A.L. Effects of Dilution on Fine Particle Mass and Partitioning of Semivolatile Organics in Diesel Exhaust and Wood Smoke; *Environ. Sci. Technol.* **2006**, *40*, 155-162.
- Robinson, A.L.; Donahue, N.M.; Shrivastava, M.K.; Weitkamp, E.A.; Sage, A.M.; Grieshop, A.P.; Lane, T.E.; Pierce, J.R.; Pandis, S.N. Rethinking Organic Aerosols: Semivolatile Emissions and Photochemical Aging; *Science* **2007**, *315*, 1259-1262.
- Cubison, M.J.; Alfarra, M.R.; Allan, J.; Bower, K.N.; Coe, H.; McFiggans, G.B.; Whitehead, J.D.; Williams, P.I.; Zhang, Q.; Jimenez, J.L.; Hopkins, J.; Lee, J. The Characterisation of Pollution Aerosol in a Changing Photochemical Environment; *Atmos. Chem. Phys.* **2006**, *6*, 5573-5508.
- Pierson, W.R.; Gertler, A.W.; Robinson, N.F.; Sagebiel, J.C.; Zielinska, B.; Bishop, G.A.; Stedman, D.H.; Zweidinger, R.B.; Ray, W.D. Real-World Automotive Emissions-Summary of Studies in the Fort McHenry and Tuscarora Mountain Tunnels; *Atmos. Environ.* **1996**, *30*, 2233-2256.
- Kirchstetter, T.W.; Harley, R.A.; Kreisberg, N.M.; Stolzenburg, M.R.; Hering, S. On-Road Measurement of Fine Particle and Nitrogen Oxide Emissions from Light and Heavy-Duty Motor Vehicles; *Atmos. Environ.* **1999**, *33*, 2955-2968.
- Stedman, D.H.; Bishop, G.A.; Aldrete, P. On-Road CO, HC, and Opacity Measurements; *7th Coordinating Research Council On-Road Vehicle Emissions Workshop*, San Diego, CA, 1997.
- Vogt, R.; Scheer, V.; Casati, R.; Benter, T. On-Road Measurement of Particle Emission in the Exhaust Plume of a Diesel Passenger Car; *Environ. Sci. Technol.* **2003**, *37*, 4070-4076.
- Bukowiecki, N.; Kittelson, D.B.; Watts, W.F.; Burtscher, H.; Weingartner, E.; Baltensperger, U. Real-Time Characterization of Ultrafine and Accumulation Mode Particles in Ambient Combustion Aerosols; *J. Aerosol Sci.* **2002**, *33*, 1139-1154.
- Kittelson, D.; Johnson, J.; Watts, W.; Wei, Q.; Drayton, M.; Paulsen, D. Diesel Aerosol Sampling in the Atmosphere. Society of Automotive Engineers (SAE) Technical Paper 2000-01-2212; SAE: Warrendale, PA, 2000.
- Seakins, P.W.; Lansley, D.L.; Hodgson, A.; Huntley, N.; Pope, F. New Directions: Mobile Laboratory Reveals New Issues in Urban Air Quality; *Atmos. Environ.* **2002**, *36*, 1247-1248.
- Kolb, C.E.; Herndon, S.C.; McManus, J.B.; Shorter, J.H.; Zahniser, M.S.; Nelson, D.D.; Jayne, J.T.; Canagaratna, M.R.; Worsnop, D.R. Mobile Laboratory with Rapid Response Instruments for Real-Time Measurements of Urban and Regional Trace Gas and Particulate Distributions and Emission Source Characteristics; *Environ. Sci. Technol.* **2004**, *38*, 5694-5703.
- Canagaratna, M.R.; Jayne, J.T.; Ghertner, D.A.; Herndon, S.; Shi, Q.; Jiménez, J.L.; Silva, P.; Williams, P.; Lanni, T.; Drewnick, F.; Demerjian, K.L.; Kolb, C.E.; Worsnop, D.R. Chase Studies of Particulate Emissions from In-Use New York City Vehicles; *Aerosol Sci. Technol.* **2004**, *38*, 555-573.
- Zavala, M.; Herndon, S.C.; Wood, E.C.; Jayne, J.; Nelson, D.D.; Trimborn, A.M.; Dunlea, E.; Knighton, W.B.; Mendoza, A.; Allen, D.T.; Kolb, C.E.; Molina, M.J.; Molina, L.T. Comparison of Emissions from On-Road Sources Using a Mobile Laboratory under Various Driving and Operational Sampling Modes; *Atmos. Chem. Phys.* **2009**, *9*, 1-14.
- Westerdahl, D.; Fruin, S.; Sax, T.; Fine, P.M.; Sioutas, C. Mobile Platform Measurements of Ultrafine Particles and Associated Pollutant Concentrations on Freeways and Residential Streets in Los Angeles; *Atmos. Environ.* **2005**, *39*, 3597-3610.
- Schneider, J.; Kirchner, U.; Borrmann, S.; Vogt, R.; Scheer, V. In Situ Measurements of Particle Number Concentration, Chemically Resolved Size Distributions and Black Carbon Content of Traffic-Related Emissions on German Motorways, Rural Roads and in City Traffic; *Atmos. Environ.* **2008**, *42*, 4257-4268.
- Schauer, J.J.; Rogge, W.F.; Hildemann, L.M.; Mazurek, M.A.; Cass, G.R.; Simoneit, B.R.T. Source Apportionment of Airborne Particulate Matter Using Organic Compounds as Tracers; *Atmos. Environ.* **2007**, *41*, 241-259.
- Rogge, W.F.; Hildemann, L.M.; Mazurek, M.A.; Cass, G.R.; Simoneit, B.R. Sources of Fine Organic Aerosol. 2. Noncatalyst and Catalyst-Equipped Automobiles and Heavy-Duty Diesel Trucks; *Environ. Sci. Technol.* **1993**, *27*, 636-651.
- Schauer, J.J.; Kleeman, M.J.; Cass, G.R.; Simoneit, B.R. Measurement of Emissions from Air Pollution Sources. 2. C1 through C30 Organic Compounds from Medium-Duty Diesel Trucks; *Environ. Sci. Technol.* **1999**, *33*, 1578-1587.
- Riddle, S.G.; Robert, M.A.; Jakober, C.A.; Hannigan, M.P.; Kleeman, M.J. Size Distribution of Trace Organic Species Emitted from Heavy-Duty Diesel Vehicles; *Environ. Sci. Technol.* **2007**, *41*, 1962-1969.
- Watson, J.G.; Chow, J.C.; Lowenthal, D.H.; Pritchett, L.C. Differences in the Carbon Composition of Source Profiles for Diesel- and Gasoline-Powered Vehicles; *Atmos. Environ.* **1994**, *28*, 2493-2505.
- Schauer, J.J. Evaluation of Elemental Carbon as a Marker for Diesel Particulate Matter; *J. Expo. Anal. Environ. Epidemiol.* **2003**, *13*, 443-453.
- Jayne, J.T.; Leard, D.C.; Zhang, X.; Davidovits, P.; Smith, K.A.; Kolb, C.E.; Worsnop, D.R. Development of an Aerosol Mass Spectrometer for Size and Composition Analysis of Submicron Particles; *Aerosol Sci. Technol.* **2000**, *33*, 49-70.
- Canagaratna, M.R.; Jayne, J.T.; Jiménez, J.L.; Allan, J.D.; Alfarra, M.R.; Zhang, Q.; Onasch, T.B.; Drewnick, F.; Coe, H.; Middlebrook, A.; Delia, A.; Williams, L.R.; Trimborn, A.M.; Northway, M.J.; DeCarlo, P.F.; Kolb, C.E.; Davidovits, P.; Worsnop, D.R. Chemical and Microphysical Characterization of Ambient Aerosols with the Aerodyne Aerosol Mass Spectrometer; *Mass Spectrom. Rev.* **2007**, *26*, 185-222.
- Zhang, Q.; Alfarra, M.R.; Worsnop, D.R.; Allan, J.D.; Coe, H.; Canagaratna, M.R.; Jiménez, J.L. Deconvolution and Quantification of Hydrocarbon-Like and Oxygenated Organic Aerosols Based on Aerosol Mass Spectrometry; *Environ. Sci. Technol.* **2005**, *39*, 4938-4952.
- Zhang, Q.; Jimenez, J.L.; Canagaratna, M.R.; Allan, J.D.; Coe, H.; Ulbrich, I.; Alfarra, M.R.; Takami, A.; Middlebrook, A.M.; Sun, Y.L.; Dzepina, K.; Dunlea, E.; Docherty, K.; DeCarlo, P.F.; Salcedo, D.; Onasch, T.; Jayne, J.T.; Miyoshi, T.; Shimojo, A.; Hatakeyama, S.; Takegawa, N.; Kondo, Y.; Schneider, J.; Drewnick, F.; Borrmann, S.; Weimer, S.; Demerjian, K.; Williams, P.; Bower, K.; Bahreini, R.; Cottrell, L.; Griffin, R.J.; Rautiainen, J.; Sun, J.Y.; Zhang, Y.M.; Worsnop, D.R. Ubiquity and Dominance of Oxygenated Species in Organic Aerosols in Anthropogenically Influenced Northern Hemisphere Mid-latitudes; *Geophys. Res. Lett.* **2007**, *34*, L13801.
- Docherty, K.S.; Stone, E.A.; Ulbrich, I.M.; DeCarlo, P.F.; Snyder, D.C.; Schauer, J.J.; Peltier, R.E.; Weber, R.J.; Murphy, S.M.; Seinfeld, J.H.;

- Grover, B.D.; Eatough, D.J.; Jimenez, J.L. Apportionment of Primary and Secondary Organic Aerosols in Southern California during the 2005 Study of Organic Aerosols in Riverside (SOAR-1); *Environ. Sci. Technol.* **2008**, *42*, 7655-7662.
39. Lanz, V.A.; Alfarra, M.R.; Baltensperger, U.; Buchmann, B.; Hueglin, C.; Prevot, A.S.H. Source Apportionment of Submicron Organic Aerosols at an Urban Site by Factor Analytical Modelling of Aerosol Mass Spectra; *Atmos. Chem. Phys.* **2007**, *7*, 1503-1524.
40. Herndon, S.; Onasch, T.B.; Wood, E.; Kroll, J.H.; Canagaratna, M.J.; Jayne, J.T.; Zvala, M.A.; Knighton, W.B.; Mazzoleni, C.; Dubey, M.K.; Ulbrich, I.M.; Jimenez, J.L.; Seila, R.; de Gouw, J.A.; de Foy, B.; Fast, J.; Molina, L.T.; Kolb, C.E.; Worsnop, D.R. Correlation of Secondary Organic Aerosol with Odd Oxygen in Mexico City; *Geophys. Res. Lett.* **2008**, *35*, L15804.
41. DeCarlo, P.F.; Dunlea, E.J.; Kimmel, J.R.; Aiken, A.C.; Sueper, D.; Crouse, J.D.; Wennberg, P.O.; Emmons, L.; Shinzuka, Y.; Clarke, A.; Zhou, J.; Tomlinson, J.; Collins, D.R.; Knapp, D.; Weinheimer, A.J.; Montzka, D.D.; Campos, T.; Jimenez, J.L. Fast Airborne Aerosol Size and Chemistry Measurements above Mexico City and Central Mexico during the MILAGRO Campaign; *Atmos. Chem. Phys.* **2008**, *8*, 4027-4048.
42. Aiken, A.C.; Salcedo, D.; Cubison, M.J.; Huffman, J.A.; DeCarlo, P.F.; Ulbrich, I.M.; Docherty, K.S.; Sueper, D.; Kimmel, J.R.; Worsnop, D.R.; Trimborn, A.; Northway, M.; Stone, E.A.; Schauer, J.J.; Volkamer, R.M.; Fortner, E.; de Foy, B.; Wang, J.; Laskin, A.; Shutthanandan, V.; Zheng, J.; Zhang, R.; Gaffney, J.; Marley, N.A.; Paredes-Miranda, G.; Arnott, W.P.; Molina, L.T.; Sosa, G.; Jimenez, J.L. Mexico City Aerosol Analysis during MILAGRO Using High Resolution Aerosol Mass Spectrometry at the Urban Supersite (t0). Part 1: Fine Particle Composition and Organic Source Apportionment; *Atmos. Chem. Phys.* **2009**, *9*, 6633-6653.
43. Onasch, T.B.; Jayne, J.T.; Herndon, S.; Worsnop, D.R.; Mlake-Lye, R.C. Chemical Properties of Aircraft Engine Particulate Exhaust Emissions; *J. Propul. Power* **2009**, *25*, 1121-1137.
44. Durant, J.L.; Ash, C.A.; Wood, E.C.; Herndon, S.C.; Jayne, J.T.; Knighton, W.B.; Canagaratna, M.R.; Trull, J.B.; Brugge, D.; Zamore, W.; Kolb, C.E. Short-Term Variation in Near-Highway Air Pollutant Gradients on a Winter Morning; *Atmos. Chem. Phys. Discuss.* **2010**, *10*, 5599-5626.
45. Cross, E.S.; Onasch, T.B.; Canagaratna, M.; Jayne, J.T.; Kimmel, J.; Yu, X.-Y.; Alexander, M.L.; Worsnop, D.R.; Davidovits, P. Single Particle Characterization Using a Light Scattering Module Coupled to a Time-of-Flight Aerosol Mass Spectrometer; *Atmos. Chem. Phys.* **2009**, *9*, 7769-7793.
46. DeCarlo, P.; Slowik, J.G.; Worsnop, D.R.; Davidovits, P.; Jimenez, J.L. Particle Morphology and Density Characterization by Combined Mobility and Aerodynamic Diameter Measurements. Part 1: Theory; *Aerosol Sci. Technol.* **2004**, *38*, 1185-1205.
47. Cross, E.S.; Slowik, J.G.; Davidovits, P.; Allan, J.D.; Worsnop, D.R.; Jayne, J.T.; Lewis, D.K.; Canagaratna, M.; Onasch, T.B. Laboratory and Ambient Particle Density Determinations Using Light Scattering in Conjunction with Aerosol Mass Spectrometry; *Aerosol Sci. Technol.* **2007**, *41*, 343-359.
48. Ban-Weiss, G.A.; Lunden, M.M.; Kirchstetter, T.W.; Harley, R.A. Measurement of Black Carbon and Particle Number Emission Factors from Individual Heavy-Duty Trucks; *Environ. Sci. Technol.* **2009**, *43*, 1419-1424.
49. Lowenthal, D.H.; Zielinska, B.; Chow, J.C.; Watson, J.G.; Gautam, M.; Ferguson, D.H.; Neuroth, G.R.; Stevens, K.D. Characterization of Heavy-Duty Diesel Vehicle Emissions; *Atmos. Environ.* **1994**, *28*, 731-743.
50. Yanowitz, J.; Graboski, M.S.; Ryan, L.B.A.; Alleman, T.L.; McCormick, R.L. Chassis Dynamometer Study of Emissions from 21 In-Use Heavy-Duty Diesel Vehicles; *Environ. Sci. Technol.* **1999**, *33*, 209-215.
51. Prucz, J.C.; Clark, N.N.; Gautam, M.; Lyons, D.W. Exhaust Emissions from Engines of the Detroit Diesel Corporation in Transit Buses: A Decade of Trends; *Environ. Sci. Technol.* **2001**, *35*, 1755-1764.
52. Tobias, H.J.; Ziemann, P.J. Compound Identification in Organic Aerosols Using Temperature-Programmed Thermal Desorption Particle Beam Mass Spectrometry; *Anal. Chem.* **1999**, *71*, 3428-3435.
53. Schneider, J.; Hock, N.; Weimer, S.; Borrmann, S.; Kirchner, U.; Vogt, R.; Scheer, V. Nucleation Particles in Diesel Exhaust: Composition Inferred from In Situ Mass Spectrometric Analysis; *Environ. Sci. Technol.* **2005**, *39*, 6153-6161.
54. Slowik, J.G.; Stanken, K.; Davidovits, P.; Williams, L.R.; Jayne, J.T.; Kolb, C.E.; Worsnop, D.R.; Rudich, Y. DeCarlo, P.; Jimenez, J.L. Particle Morphology and Density Characterization by Combined Mobility and Aerodynamic Diameter Measurements. Part 2: Application to Combustion Generated Soot Aerosols as a Function of Fuel Equivalence Ratio; *Aerosol Sci. Technol.* **2004**, *38*, 1206-1222.
55. Park, K.; Cao, F.; Kittelson, D.; McMurry, P. Relationship between Particle Mass and Mobility for Diesel Exhaust Particles; *Environ. Sci. Technol.* **2003**, *37*, 577-583.
56. Morawska, L.; Jamriska, M.; Thomas, S.; Ferreira, L.; Mengersen, K.; Wraith, D.; McGregor, F. Quantification of Particle Number Emission Factors for Motor Vehicles from On-Road Measurements; *Environ. Sci. Technol.* **2005**, *39*, 9130-9139.
57. Ulbrich, I.M.; Canagaratna, M.R.; Zhang, Q.; Worsnop, D.R.; Jimenez, J.L. Interpretation of Organic Components from Positive Matrix Factorization of Aerosol Mass Spectrometric Data; *Atmos. Chem. Phys.* **2009**, *9*, 2891-2918.
58. Ban-Weiss, G.A.; McLaughlin, J.P.; Harley, R.A.; Lunden, M.M.; Kirchstetter, T.W.; Kean, A.J.; Strawa, A.W.; Stevenson, E.D.; Kendall, G.R. Long-Term Changes in Emissions of Nitrogen Oxides and Particulate Matter from On-Road Gasoline and Diesel Vehicles; *Atmos. Environ.* **2008**, *42*, 220-232.
59. Zhang, Q.; Worsnop, D.R.; Canagaratna, M.R.; Jimenez, J.L. Hydrocarbon-Like and Oxygenated Organic Aerosols in Pittsburgh: Insights into Sources and Processes of Organic Aerosols; *Atmos. Chem. Phys.* **2005**, *5*, 3289-3311.
60. Kleinman, L.I.; Springston, S.R.; Wang, J.; Daum, P.H.; Lee, Y.-N.; Nunnermacker, L.J.; Senum, G.I.; Weinstein-Lloyd, J.; Alexander, M.L.; Hubbe, J.; Ortega, J.; Zaveri, R.A.; Canagaratna, M.R.; Jayne, J. The Time Evolution of Aerosol Size Distribution over the Mexico City Plateau; *Atmos. Chem. Phys.* **2009**, *9*, 4261-4278.
61. Miyakawa, T.; Takegawa, N.; Kondo, Y. Photochemical Evolution of Submicron Aerosol Chemical Composition in the Tokyo Megacity Region in Summer; *J. Geophys. Res.* **2008**, *113*, D14304.
62. Alfarra, M.R.; Coe, H.; Allan, J.D.; Bower, K.N.; Boudries, H.; Canagaratna, M.R.; Jimenez, J.L.; Jayne, J.T.; Garforth, A.A.; Li, S.M.; Worsnop, D.R. Characterization of Urban and Rural Organic Particulate in the Lower Fraser Valley Using Two Aerodyne Aerosol Mass Spectrometers; *Atmos. Environ.* **2004**, *38*, 5745-5758.

#### About the Authors

Manjula R. Canagaratna, Timothy B. Onasch, and Scott C. Herndon are principal scientists; Eben S. Cross is a postdoctoral fellow; John T. Jayne is a co-director of the Center for Aerosol and Cloud Chemistry; Richard C. Mlake-Lye is the director of the Center for Aero-Thermodynamics; Charles E. Kolb is president of Aerodyne Research, Inc.; and Douglas R. Worsnop is a vice president and co-director of the Center for Aerosol and Cloud Chemistry, all at Aerodyne Research, Inc. Ezra C. Wood was a senior scientist at Aerodyne Research, Inc., during this work and is currently affiliated with the Department of Public Health, University of Massachusetts, Amherst, MA. Please address correspondence to: Manjula R. Canagaratna, Aerodyne Research, Inc., Center for Atmospheric and Cloud Chemistry, 45 Manning Road, Billerica, MA 01983; phone: +1-978-887-5060, extension 285; fax: +1-978-663-4918; e-mail: mrcana@aerodyne.com